

Electron Transfer from the Water Oxidizing Complex at Cryogenic Temperatures: The S₁ to S₂ Step[†]

Jonathan H. A. Nugent,* Irine P. Muhiuddin, and Michael C. W. Evans

Department of Biology, Darwin Building, University College London, Gower Street, London WC1E 6BT, U.K.

Received June 25, 2001; Revised Manuscript Received January 22, 2002

ABSTRACT: We report the detection of a “split” electron paramagnetic resonance (EPR) signal during illumination of dark-adapted (S₁ state) oxygen-evolving photosystem II (PSII) membranes at <20 K. The characteristics of this signal indicate that it arises from an interaction between an organic radical and the Mn cluster of PSII. The broad radical signal decays in the dark following illumination either by back-reaction with Qa^{•−} or by forward electron transfer from the Mn cluster. The forward electron transfer (either from illumination at 11 K followed by incubation in the dark at 77 K or by illumination at 77 K) results in the formation of a multiline signal similar to, but distinct from, other well-characterized multiline forms found in the S₀ and S₂ states. The relative yield of the “S₁ split signal”, which we provisionally assign to S₁X[•], where X could be Y_Z[•] or Car^{•+}, and that of the 77 K multiline signal indicate a relationship between the two states. An approximate quantitation of the yield of these signals indicates that up to 40–50% of PSII centers can form the S₁ split signal. Ethanol addition removes the ability to observe the S₁ split signal, but the multiline signal is still formed at 77 K. The multiline forms with <700 nm light and is not affected by near-infrared (IR) light, showing that we are detecting electron transfer in centers not responsive to IR illumination. The results provide important new information about the mechanism of electron abstraction from the water oxidizing complex (WOC).

PSII¹ is the membrane–protein complex which catalyzes electron transfer from water to plastoquinone (1–3). The PSII complex consists of more than 25 proteins and several different active cofactors, including the manganese site that is required for water oxidation. PSII electron transfer begins with the excitation of the reaction center multi-chlorophyll *a* species P680, to P680*, and rapid electron transfer from P680*, via pheophytin, to the bound plastoquinone, Qa, to form P680⁺ Qa^{•−}. Electron transfer then occurs from Qa^{•−} to a second plastoquinone, Qb. Following two turnovers, Qb has accepted two electrons and taken up two protons. QbH₂ dissociates from its site into the membrane pool of plastoquinone. A non-heme iron, which can be oxidized under some conditions but is usually present as Fe²⁺, is situated between Qa and Qb.

P680⁺ extracts an electron from the WOC via the electron donor Y_Z, tyrosine-161 on the D1 polypeptide, to form Y_Z[•], the neutral tyrosine radical (1–3). Y_D, tyrosine-161 on the

D2 polypeptide, cytochrome *b*-559 (Cyt *b*-559), Chl Z, and a carotenoid can be secondary electron donors to oxidized P680 under some conditions (1–3). The reduction kinetics of P680⁺ by Y_Z and subsequently of Y_Z[•] by the WOC is dependent on the S-state. A large fraction of P680⁺ is reduced by Y_Z in nanoseconds but slower phases occur (4–6). To explain the slower phases, we suggested a role for proton-coupled electron transfer processes in which net deprotonation from the region is required to complete reduction of P680⁺, resulting in a progressive change in the equilibrium between Y_Z/Y_Z[•] and P680/P680⁺ toward Y_Z[•] formation (5, 7). Y_Z has been proposed to be involved in the water oxidation process itself, as a hydrogen atom abstractor or in promoting proton-coupled electron transfer from the WOC (1–3, 7–14).

During one cycle to oxidize two molecules of water to oxygen and protons, the WOC passes through redox states termed S-states, electrons being removed on each step from S₀ to S₄ and O₂ being evolved at the transient S₄ state, during S₃–S₀ (1–3, 15, 16). Four Mn atoms are thought to be involved in the WOC. Oxidation of the WOC must be an almost electroneutral process with proton release to the lumen during the S-state cycle providing the necessary charge balance to electron transfer.

The dark stable state of PSII is S₁. After a few minutes in the dark, about 75% of PSII is in S₁ and 25% in S₀. During further dark adaptation, the S₀ state is slowly oxidized to S₁ by Y_D[•] (1–3). Y_D[•] can also be reduced by Qa^{•−} on storage at cryogenic temperatures (3). The S₂ and S₃ states are unstable with short half-lives (<30 s) at room temperature, decaying back to S₁ (1–3). The lifetimes of S₂ and S₃ increase at lower temperatures, recombination with reduced

[†] Financial assistance from the U.K. Biotechnology and Biological Sciences Research Council and the Leverhulme Trust is acknowledged. J.H.A.N. and M.C.W.E. are members of the Bloomsbury Centre for Structural Biology at UCL and Birkbeck College.

* Corresponding author. Fax: +44 (0)20 7679 7096. E-mail: j.nugent@ucl.ac.uk. Phone: +44 (0)20 7679 2681.

¹ Abbreviations: EPR, electron paramagnetic resonance spectrometry; DCMU, 3-(3,4-dichlorophenyl)-1,1-dimethylurea; PPBQ, phenyl-1,4-benzoquinone; DCBQ, 2,5-dichlorobenzoquinone; WOC, water oxidizing complex; PSII, photosystem II; MES, 2-(*N*-morpholino)-ethanesulfonic acid; Chl, chlorophyll; Qa, first PSII plastoquinone electron acceptor; Qb, second PSII plastoquinone electron acceptor; Y_Z, tyrosine D1 161 (Y_Z[•] when oxidized); Y_D, tyrosine D2 161 (Y_D[•] when oxidized); Cyt *b*-559, cytochrome *b*-559; P680, PSII primary electron donor; FCCP, carbonyl cyanide *p*-(trifluoromethoxy)phenylhydrazide; IR, infrared.

Qa being very slow at 200 K. The Mn valence states during the S-state cycle are not known, but models with the S₂ state having 3Mn³⁺ 1Mn⁴⁺ or 1Mn³⁺ 3Mn⁴⁺ are the main alternatives discussed (1–3, 17). When and where water binding occurs is not known. Recent studies show that there is interaction between water and the WOC before S₃, with significant differences in the binding of the two water molecules (18, 19). A number of EPR signals have been used to study the S-states. EPR signals are detected from the S₀ (20–22), S₁ (23–26), S₂ (27–30), and S₃ states (31–33). These are consistent with Mn oxidation during S₀ to S₁ to give a Mn³⁺/Mn³⁺ dimer and during S₁ to S₂ to give a Mn³⁺/Mn⁴⁺ dimer, but the oxidation of Mn or a ligand is still debated for S₂ to S₃. The addition of methanol is required to observe the S₀ S = 1/2 multiline signal. S₂ EPR signals include an S = 1/2 multiline signal centered on *g* = 2 (27, 28) and an S ≥ 3/2 signal at *g* = 4.1 (29, 30). The latter is present in sucrose-containing samples but is removed by alcohols such as methanol. The *g* = 4.1 signal can be formed from the multiline signal via an S = 5/2 state by using IR illumination at <150 K (34–37). The S₁ (*g* = 4.8 or 12) and S₃ states are characterized by weak integer spin signals observed by parallel mode EPR (23–26, 32, 33).

Y_Z is close to the Mn cluster (38–41), and when both are paramagnetic, i.e., Y_Z[•] plus a paramagnetic Mn cluster, they can interact to give complex broad electron paramagnetic resonance (EPR) “split” signals at cryogenic temperatures. The split EPR signals from the WOC were initially reported in samples where oxygen evolution was inhibited at the S₂ to S₃ step (42–44). These signals are now assigned to a S₂Y_Z[•] state (45–47).

We have already reported experiments that suggested that an interaction between an organic radical (probably Y_Z[•]) and the Mn cluster (S₂Y_Z[•]) could be observed in uninhibited PSII and that this is related to formation of S₃ (31). These observations have been extended by Petrouleas and co-workers (33), additionally showing that IR illumination of the S₃ state forms the same state (S₂Y_Z[•]).

In this study we find evidence that the S₁ to S₂ step can operate at very low temperatures. We show the characterization of a signal attributed to the interaction between paramagnetic S₁ and X[•] (where X = Y_Z or carotenoid) as an intermediate state between the S₁ and S₂ states. The results showing that a substantial number of centers are able to advance to S₂ at very low temperatures confirm the unusual temperature profile of this step. Preliminary results from this work are found in refs 48 and 49.

MATERIALS AND METHODS

PSII membranes were prepared from market spinach or freshly cropped 10–14-day-old pea seedlings using Triton X-100, with the modifications of Ford and Evans (50). Reagents used were all analytical grade. Chlorophyll (Chl) concentration was measured by the method of Porra (51). Control rates of oxygen evolution for PSII membranes were 400–1000 μmol of O₂ (mg of Chl)^{−1} h^{−1} (the lower rates were obtained in large-scale spinach preparations) using ferricyanide and dimethylbenzoquinone as electron acceptors and measured in a Clark-type oxygen electrode at 298 K. The membranes were stored at 77 K in 20 mM 2-(*N*-morpholino)ethanesulfonic acid (MES), 15 mM NaCl, and

5 mM MgCl₂, pH 6.5, plus cryoprotectant (buffer A). Sucrose (0.4 M) or 20–25% v/v glycerol was used as a cryoprotectant as discussed in the Results section. Before preparation of EPR samples, the PSII membranes were (except where stated) washed in buffer A containing 2 mM ethylenediaminetetraacetic acid to remove adventitiously bound Mn²⁺, followed by centrifugation and resuspension in 20 mM MES, 15 mM NaCl, 4 mM MgCl₂, and 1 mM CaCl₂, pH 6.5, plus cryoprotectant (0.4 M sucrose or 20–25% v/v glycerol). Removal of Mn from the WOC was achieved using Tris washing at high pH as given in ref 31.

For EPR, 0.3–0.4 mL samples (approximately 6–10 mg of Chl/mL; 25–40 μM PSII) were placed in calibrated ~3 mm quartz EPR tubes. Identical sets of samples in calibrated EPR tubes were made for each experiment, using the same preparation and chlorophyll concentration. They were given a brief (30 s) illumination at 277 K to turnover the PSII reaction center and restore Y_D[•] lost on storage. Further procedures were carried out in the dark or under a dim green light.

Samples were dark adapted for 3 h at 273 K and then treated as described in the text and figure legends. Additions of 0.5 mM 3-(3,4-dichlorophenyl)-1,1-dimethylurea (DCMU), 0.5–1 mM 2,5-dichlorobenzoquinone (DCBQ), phenyl-1,4-benzoquinone (PPBQ), or 0.25 mM carbonyl cyanide *p*-(trifluoromethoxy)phenylhydrazone (FCCP) were made from freshly made concentrated stock solutions in dimethyl sulfoxide (maximum final concentration 1%). Ethanol or methanol was used at 2.5% final concentration. Treated or untreated samples were then dark adapted for a further 30 min on ice before being frozen to 77 K in the dark (total dark adaptation 4 h). This produced samples initially in the S₁ Qa state, as indicated by the absence of the S₂ EPR markers, the multiline signal or the *g* = 4.1 signal, and Qa^{•−}. Absence of photosystem I was confirmed by the lack of signals from oxidized P700 or reduced iron–sulfur centers A or B following illumination at <30 K. The signals present in control samples (Cyt *b*-559 etc.) were directly compared during experiments that involved EPR data collection on different days. This confirmed the reproducibility of spectra so that no normalization was required or performed. Precautions to exclude signals from oxygen were as previously described (31). Careful wiping of the tubes prior to insertion into the cryostat also helps to prevent frozen oxygen from condensing on the tube or sample surface and thereby distort spectra.

During experiments, samples were illuminated at a variety of temperatures. Illumination in the EPR cavity at <30 K used a 150 W light source and fiberoptic light guide, while other illumination used a 1000 W light source, protecting the sample from heating where necessary by a 5 cm water filter. IR light was excluded from illuminated samples where stated by using an Ealing electrooptics long-wavelength cutoff filter (50% transmission at 661.6 nm, ~0 above 700 nm). Samples for 77 K dark adaptation or illumination were placed in liquid nitrogen in a silvered dewar, while samples for 200 K illumination were incubated using an ethanol/dry ice bath in an unsilvered clear glass dewar. The temperature of the bath was measured by thermometer. Temperatures within the EPR cryostat were measured with a calibrated thermocouple beneath the sample. Once the cryostat temperature reached equilibrium, the temperature could be

maintained within ± 0.1 K for several hours if required. At <20 K any slight changes caused by heating during illumination were reversed by the helium flow in less than 1 min. Heating effects due to illumination have been studied and minimized by (a) monitoring the effect of illumination on the signal size of other more stable signals over the several years we have used this cryostat/illumination combination, (b) specific measurements on the S₁ split signal at various helium flow rates and light intensity (scale 0–10 on light source), and (c) use of an IR filter to eliminate heating effects completely (this was not used routinely as it could only be crudely placed in front of the cavity, resulting in the light guide being further away from the sample and thus reducing the light intensity at the sample). In some cases spectra from illuminated samples were recorded a short time (usually 1 min) after illumination to check for heat-induced effects. Heat-induced effects can easily be detected and roughly quantitated as a sudden change in signal size when the light is turned on or off.

Samples were examined by EPR at cryogenic temperatures using a JEOL RE1X spectrometer fitted with an Oxford Instruments cryostat. EPR conditions are given in the figure legends. Spectra were recorded and manipulated using a Dell microcomputer running Asyst software and spectra plotted using Microsoft Excel. No filtering, smoothing, fitting, or background subtractions were used. Difference spectra were obtained only from subtraction of spectra from the same sample. The vertical scale in figures showing first derivative EPR spectra is arbitrary, with spectra at the same instrument gain unless stated in the figure legend. The field scale corresponds to *g*-values as follows: *g* = 6 at 107.6 mT, *g* = 3 at 215.2 mT, and *g* = 2 at 322.8 mT. S₂ multiline signal intensities were determined as peak to trough heights, using six peaks, three above and three below *g* = 2, away from interference caused by overlap of other PSII signals. The S₂ yield was compared to that achieved by illumination of an S₁ sample at 200 K for 15 min. S₀ was prepared using hydroxylamine as in ref 20. The amplitude of split *g* = 2 signals was measured as the peak to trough height from the light on minus dark difference spectrum.

RESULTS

The basic EPR properties of dark-adapted PSII membranes (S₁) at cryogenic temperatures have been studied in a number of laboratories and are well established (e.g., ref 52). A number of electron transfer reactions are possible, even following illumination at temperatures below 77 K. Below 200 K, it is generally accepted that only a single turnover of the PSII reaction center can occur, the electron transfer forming Qa^{•−} and one of several oxidized species, either S₂, oxidized Cyt *b*-559, monomeric Chl Z⁺, or, as confirmed recently, carotenoid (53, 54). At 77 K and below, the secondary donors usually form the major oxidized product. At 200 K, S₂ is the major product, giving either the multiline EPR signal and/or (dependent on the cryoprotectant and sample additions used) the *g* = 4.1 form of S₂ (1–3, 17, 27–30).

We have now found that illumination of PSII membranes, poised in the S₁ state by dark adaptation, in the EPR cavity at <20 K results in a change close to the *g* = 2 organic radical region (Figure 1, upper panel). Figure 1A shows the

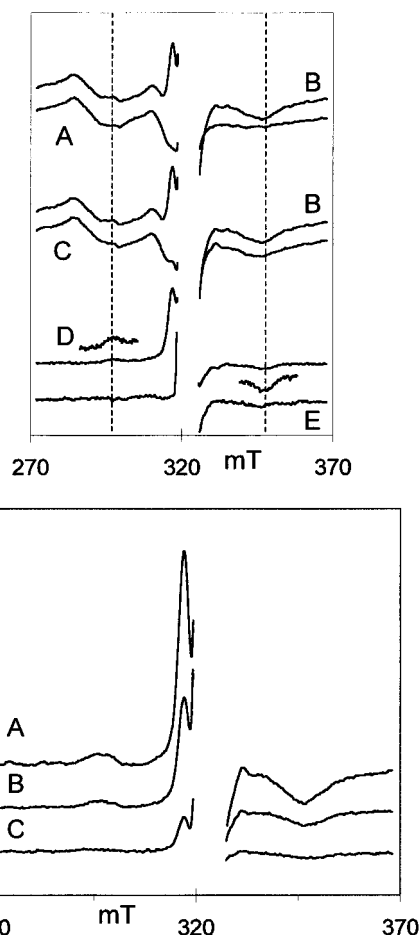


FIGURE 1: EPR spectra showing the formation and decay of the S₁ split signal at 11 K. Upper panel: (A) Dark-adapted spinach PSII membranes in the S₁ state containing 0.5 mM PPBQ (see Materials and Methods) at 8 mg of Chl/mL. (B) Sample as in (A), illuminated at 11 K in the spectrometer. (C) Sample shown in (B) after 15 min in the dark at 11 K following illumination at 11 K. (D) Sample reilluminated at 11 K minus decayed difference spectrum (C), showing the line shape of the signal. The weak outer lines, indicated by the dotted lines, have been expanded for clarity. (E) Sample illuminated at 11 K minus dark difference spectrum of a Tris-washed PSII sample showing the absence of the S₁ split signal in Mn-depleted samples. EPR conditions: temperature 11 K, modulation amplitude 1.6 mT, and microwave power 10 mW. The large *g* = 2 organic radical peak has been omitted. Lower panel: Sample illuminated at 11 K minus dark difference spectra of spinach PSII membranes at 8 mg of Chl/mL in the S₁ state containing 0.67 mM DCBQ (see Materials and Methods). (A) Microwave power 50 mW. (B) Microwave power 10 mW. (C) Microwave power 1 mW. Other EPR conditions as in upper panel.

EPR spectrum near *g* = 2 of dark-adapted PSII membranes and the spectrum following illumination at 11 K (Figure 1B). A narrow signal appears near 317 mT (*g* = 2.035), together with a broad peak at 330–345 mT. Illumination at this temperature in the EPR cavity results in electron transfer to Qa in some PSII reaction centers, accounting for the broad signal, which is known as the *g* = 1.9 form of Qa^{•−} iron semiquinone. The narrow signal near 317 mT is novel. Oxidized secondary electron donors such as chlorophyll or Cyt *b*-559 only show a very slow recombination with Qa^{•−} during storage at 77 K, the decay of the carotenoid radical is faster than chlorophyll or Cyt *b*-559 (52–55), and its possible involvement will be discussed later. The signal near 317 mT formed by illumination (Figure 1B) decays in minutes at 11 K, such that after 15 min in the dark at 11 K

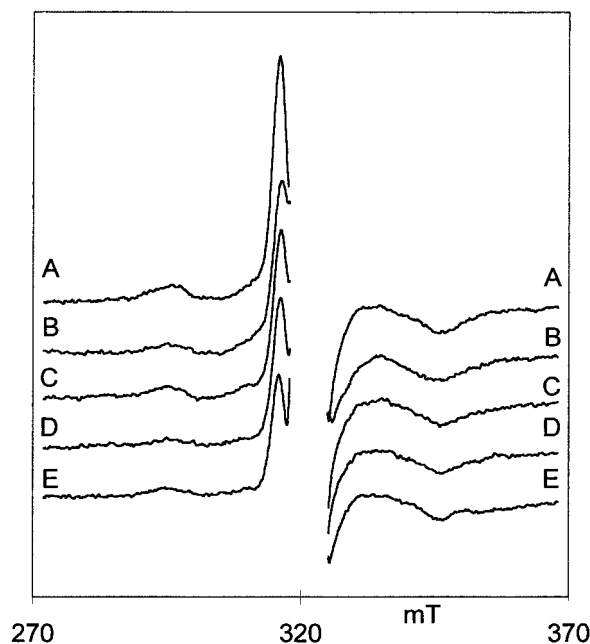


FIGURE 2: EPR spectra showing the formation of the S1 split signal at 8 K following various treatments. Dark-adapted pea PSII membranes in the S_1 state (see Materials and Methods) at 6.1 mg of Chl/mL were illuminated in the spectrometer cavity at 8 K. The traces shown are the difference spectra between the spectrum following illumination and the dark-adapted S_1 state spectrum taken before illumination. All samples except (B) contain sucrose as cryoprotectant. (A) Sample containing 0.5 mM DCBQ (in DMSO). (B) Untreated sample containing glycerol as cryoprotectant. (C) Sample containing 1% DMSO. (D) Sample containing 0.25 mM FCCP (in DMSO). (E) Sample containing 0.25 mM DCMU (in DMSO). EPR conditions: temperature 8 K, modulation amplitude 1.6 mT, and microwave power 10 mW. See Materials and Methods for further details.

(Figure 1C), the signal has decayed almost completely, while only part of the $Qa^{\bullet-}$ signal has decayed. Further illumination at 11 K restores the $g = 2$ signal. The light-induced difference spectrum is shown (Figure 1D). The peak near $g = 2$ is accompanied by weak outer lines, equidistant from $g = 2$, which on careful inspection can be distinguished from the signals of $Qa^{\bullet-}$ and Cyt b -559 which overlap this region, although a contribution from $Qa^{\bullet-}$ is always present. The g_y peak of Cyt b -559 (near 290 mT) present in the dark-adapted sample does not change on illumination while the Cyt b -559 g_y peak formed upon illumination (at slightly higher field) does not decay over a short time scale at this temperature. It is more difficult to separate the weak high-field peak due to the overlap with the $Qa^{\bullet-}$ signal. The new signal was not observed in Mn-depleted samples (Figure 1E). The removal of the Mn cluster causes other changes in PSII, e.g., oxidation of Cyt b -559, which limit electron transfer at <20 K.

Temperature and power saturation studies show that the signal saturates at high levels of microwave power, i.e., at >1 mW at 5 K and >10 mW at 11–12 K, indicating the involvement of a transition metal in one of the interacting species. Figure 1 (lower panel) shows how the signal increases with microwave power. The temperature dependence of the signal is more difficult to assess as it is not stable, and therefore the yield is affected by the temperature dependence of the electron transfer, in addition to any temperature characteristics of the signal. The yield of $Qa^{\bullet-}$ by illumination decreases between illumination at 77 and

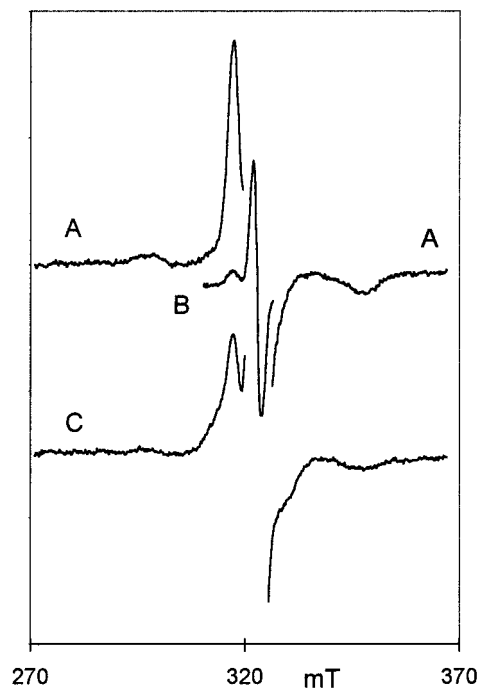


FIGURE 3: EPR spectra showing the line shape of the S1 split signal. (A) Dark-adapted pea PSII membranes in the S_1 state (see Materials and Methods) at 9.6 mg of Chl/mL were illuminated in the spectrometer cavity at 6.7 K and then kept at 6.7 K for 25 min in the dark until the S1 split signal had decayed. The sample was then illuminated again at 6.7 K. The traces shown are the difference spectra between the spectrum following reillumination at 6.7 K and the spectrum after 25 min in the dark taken before reillumination. (A) Sample containing 1 mM DCBQ. (B) Sample as in (A) at lower instrument gain to show the difference spectrum at $g = 2$. (C) Sample containing 0.25 mM FCCP. EPR conditions: temperature 6.7 K, modulation amplitude 1.25 mT, and microwave power 5 mW.

5–20 K in the EPR cavity (e.g., ref 56), confirming this restriction of electron transfer by lowering the temperature.

The light-induced signal resembles the type of signal formed by interaction between two spin systems and will be referred to as the “S1 split signal”. The interaction appears to be between a $g = 2$ radical system weakly coupled (exchange or dipolar or both) to another spin from its similarity to the interactions that occur between Y_Z and Mn and pheophytin, I, and the iron semiquinone in PSII (38–41). The signal is observed in untreated PSII membranes, but changing the cryoprotectant from sucrose to glycerol or the use of a variety of added compounds increases the yield (Figure 2). These compounds include dimethyl sulfoxide (the solvent used for many organic chemical additions to PSII) and, in addition to the effect of DMSO, FCCP and quinones such as PPBQ or DCBQ (Figure 2). The additions of PPBQ and DCBQ also cause a dark oxidation of some Cyt b -559, while FCCP is known to cause autooxidation of Cyt b -559 and reduce Y_D^{\bullet} (56). The decrease in amounts of competing secondary donors could explain an increase in the yield of the S1 split signal caused by these additions. The addition of the herbicide DCMU, which displaces Q_b , does not affect the S1 split signal (Figure 2E).

The line shape observed with FCCP is slightly different from that seen with other additions such as exogenous quinones (Figure 3). Figure 3 shows the light-induced difference spectra of PSII membranes containing 1 mM

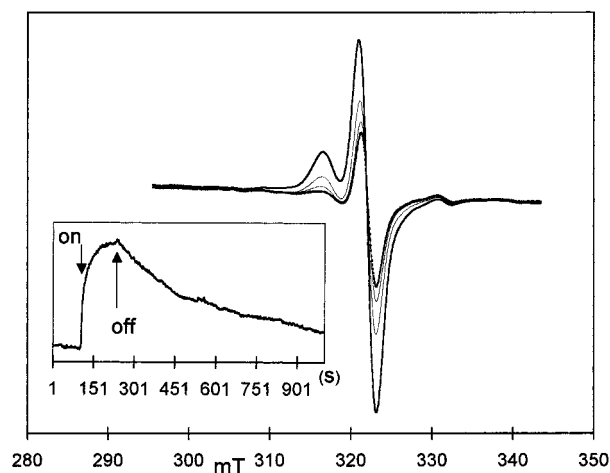


FIGURE 4: EPR spectra showing the line shape of the S₁ split signal at $g = 2$ and the kinetics of decay of the signal at 11 K. The main figure shows the spectrum near $g = 2$ of a sample of spinach PSII membranes (8 mg of Chl/mL) containing 0.5 mM PPBQ. The sample was illuminated, then dark adapted for 30 min at 8.5 K, and then reilluminated at 8.5 K in the spectrometer, and successive scans were taken after turning off the illumination to show the decay of the signal. The scans were taken immediately after illumination (outer bold line), 220 and 520 s after illumination (faint lines), and 830 s after illumination (inner bold line). EPR conditions: temperature 8.5 K, modulation amplitude 1.6 mT, and microwave power 100 mW. Inset: Kinetics of decay of the S₁ split signal at 317 mT. The sample of PSII membranes (8 mg of Chl/mL) contained 0.75 mM DCBQ. The sample was treated as in the main figure and then reilluminated. The illumination began at 100 s, the light was turned off at 240 s, and the decay was monitored. EPR conditions: temperature 11 K, modulation amplitude 1.6 mT, and microwave power 10 mW.

DCBQ (A and B) or 250 μ M FCCP (C), obtained by subtracting the spectrum taken 25 min following illumination from that during illumination. The broader line in the FCCP sample can be compared with the usual line shape seen with no addition, DCBQ, or other additions. In Figure 3B, which resolves the $g = 2$ region, the peak of the split signal observed in Figure 1 (to the low field of $g = 2$) is revealed as a satellite line of a larger peak superimposed on the organic radical peaks at $g = 2$ (see also Figure 4).

Figure 4 shows the kinetics of decay of the S₁ split signal (at 317 mT) following illumination (inset). The spectrum at $g = 2$ is shown immediately following illumination (bold outer line) and then during decay in the dark, at approximately 220 and 520 s following illumination in fainter lines and then at 830 s in the bold inner line. At 323 mT some carotenoid or chlorophyll radical has been induced by the illumination. Although nearly all of this remains after the S₁ split signal has decayed, some slow decay of these species may contribute to the decay kinetics, so that the kinetic trace is taken at 317 mT to minimize the influence of other species. At 317 mT the $t = 1/2$ is 230 s in this experiment at 11 K.

It was observed in some samples, e.g., samples with glycerol as cryoprotectant, that the yield of the S₁ split signal fell significantly during illumination in the EPR cavity. This led to the finding that another signal could be formed apparently at the expense of the S₁ split signal. Figure 5 shows this process in sucrose samples where the split signal is more stably formed at <10 K and the transition can be studied more easily. Figure 5 shows that a short period of

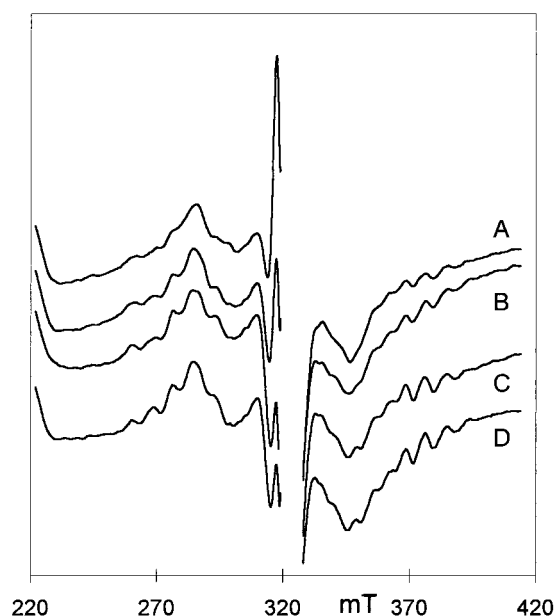


FIGURE 5: EPR spectra showing loss of the S₁ split signal and generation of a multiline signal. The sample of pea PSII membranes (7.7 mg of Chl/mL) contained 1 mM DCBQ and was in the S₁ state following dark adaptation as given in Materials and Methods. The spectra show the sample during illumination at 6.7 K in the spectrometer. The spectrum of the dark-adapted sample is as in Figure 6A. (A) First illumination at 6.7 K. (B) Second illumination at 6.7 K of the sample in (A) following 2 min at 77 K in the dark. (C) Sample as in (A), illuminated twice at 6.7 K followed each time by 2 min at 77 K in the dark. The spectrum shows the third illumination at 6.7 K. (D) Duplicate sample illuminated by <700 nm light for 10 min at 77 K and then illuminated in the spectrometer at 6.7 K. EPR conditions: temperature 6.7 K, modulation amplitude 2 mT, and microwave power 10 mW.

darkness at 77 K following illumination in the EPR cavity at 6.7 K decreased the yield of the S₁ split signal on subsequent illumination at 6.7 K and caused a multiline-type signal to appear (Figure 5B). A small amount of this multiline signal was also formed during the illumination in the cavity (Figure 5A). A subsequent short dark period at 77 K following a second illumination at 6.7 K further decreased the split signal and increased the multiline signal (Figure 5C). Illumination of a dark-adapted PSII membrane sample directly at 77 K with white light through a 700 nm cutoff filter (to eliminate IR light) produced an identical multiline-type signal (now referred to as the "77 K multiline signal") and a decrease in the yield of the S₁ split signal upon subsequent illumination at <10 K (Figure 5D). The inverse relationship between the yield of the 77 K multiline signal and the S₁ split signal was confirmed in several preparations. In glycerol-containing samples the formation of the multiline signal at the expense of the split signal occurs more easily at <20 K (not shown), explaining the gradual decrease in the yield of the S₁ split signal during illumination at <20 K in these samples. The 77 K multiline signal is characterized by a rather uneven distribution of peak sizes and stronger outer lines (see Figure 9). The line shape is therefore slightly different from other multiline signals. This may be due to many causes, such as the inability of the structure to relax fully at 77 K.

The multiline signal was more stable than the S₁ split signal but did decay slowly on storage at 77 K in the dark as shown in Figure 6. Figure 6A shows the spectrum of dark-

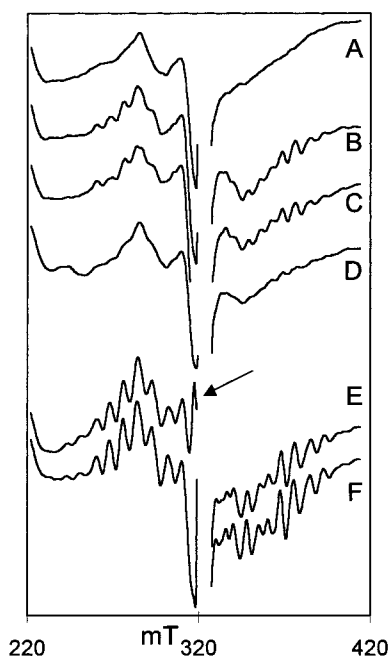


FIGURE 6: EPR spectra showing the generation of a multiline signal by illumination at cryogenic temperatures. The sample of pea PSII membranes (7.7 mg of Chl/mL) contained 1 mM DCBQ and was in the S_1 state following dark adaptation as given in Materials and Methods. (A) Dark-adapted sample. (B) Sample as in (A) following illumination at 6.7 K and a dark period (15 min) at 77 K. (C) Duplicate sample to that in (A) following illumination at 77 K for 10 min with <700 nm light. (D) Sample as in (B) following storage at 77 K in the dark for 48 h. (E) Sample as in (F) after storage for 5 days at 77 K in the dark following 200 K illumination. The spectrum was recorded under illumination at 7 K in the spectrometer; the split signal formed is indicated with an arrow. (F) Sample as in (D) after illumination at 200 K for 15 min. EPR conditions: temperature (A–D) 6.7 K and (E, F) 7 K, modulation amplitude 2 mT, and microwave power 10 mW.

adapted PSII membranes containing DCBQ while Figure 6B,C shows the multiline signal formed by illumination in the cavity followed by a short period at 77 K in the dark (Figure 6B) or by illumination at 77 K with <700 nm light (Figure 6C). After storage for 2 days at 77 K in the dark, the multiline and part of the Qa^+ signal had decayed (Figure 6D). The S_1 split signal was observed in increased yield on illumination at <10 K compared to that before storage (not shown).

Storage of a sample identical to that in Figure 6A–D at 77 K following 200 K illumination to yield the S_2 state multiline results in partial decay of the S_2 multiline (57), and subsequent illumination of the sample at <10 K produces a small split signal (Figure 6E, arrow). Figure 6F shows the yield of the S_2 state multiline signal observed following subsequent 200 K illumination.

Although the line shape of the 200 K multiline form is slightly different from that of the “77 K multiline”, it is possible to make an approximate measurement of yield by comparison of peaks from each spectrum as given in Materials and Methods. In the most favorable cases the yield of the 77 K multiline signal obtained as in Figures 6B and 6C reaches about 25–30% of the yield of the S_2 multiline formed by 200 K illumination. The yield of the S_1 split signal (measured using the illuminated minus dark difference spectrum), in samples showing $\sim 25\%$ yield of multiline, falls to about 40% of its initial value. This indicates that up to

40–50% of PSII centers able to generate an S_2 multiline at 200 K can form an S_1 split signal in these samples.

Treatment of PSII membranes with alcohols such as ethanol and methanol is known to modify the signal arising from the Mn cluster of the WOC (1–3, 17, 37). Addition of 1–3% methanol or 2.5% ethanol to PSII membranes was shown to remove the ability to observe the S_1 split signal but not the production of the 77 K multiline state (Figure 7). Figure 7 shows the spectra obtained from PSII membranes containing 2.5% ethanol and 1 mM DCBQ (box a, left side) compared to PSII membranes containing 1 mM DCBQ (box b, right side). Figure 7C,H shows the spectrum of dark-adapted PSII. Illumination at 6.7 K produces the S_1 split signal in the control (Figure 7F) but not in the ethanol sample (Figure 7A). In contrast, illumination with <700 nm light at 77 K induces a 77 K multiline signal in both types of samples (Figure 7B,G). Addition of 2.5% methanol also completely removes the ability to form the S_1 split signal but also has a general effect on PSII, substantially decreasing the degree of charge separation obtained at cryogenic temperature (not shown).

A feature of the Mn cluster in PSII membranes is the response to near-IR light. This causes the formation of a $g = 4.1$ form of S_2 at the expense of the S_2 multiline, via a number of intermediate states which can be trapped at cryogenic temperatures (34–37), and has also been shown to affect the Mn cluster in the S_1 and S_3 states (33, 58). The IR light, which cannot cause a charge separation in the reaction center, is thought to affect an Mn^{3+} atom within the cluster, causing a change in valence distribution within the cluster or a spin transition in the Mn^{3+} atom (34, 36, 59). Illumination of PSII membranes with unfiltered white light containing IR at 77 K produced a $g = 4.1$ S_2 signal in low yield as expected, showing that some PSII centers are affected by IR light. Identical samples, which gave the S_1 split signal on illumination at 10 K (Figure 8A), were illuminated at 77 K with <700 nm light to produce the 77 K multiline signal (Figure 8B). Further illumination of the 77 K multiline signal in either DCBQ or ethanol DCBQ samples (Figure 7D,I) with unfiltered white light at 77 K did not significantly affect the 77 K multiline signal yield (Figure 7E,J), showing that IR illumination does not affect the 77 K multiline. The unfiltered white light does produce some additional $g = 4.1$ signal (Figure 8C), showing that the 77 K multiline and $g = 4.1$ signals are formed in different PSII centers.

Figure 9 compares multiline line shapes. Because of the instability of the 77 K multiline and its decay by recombination with Qa^+ , it was not possible to obtain a spectrum that did not contain an underlying contribution from Qa^+ to high field of $g = 2$ (330–375 mT). However, the line shape is clearly distinct from that of S_2 (Figure 9A) and S_0 (Figure 9D), the latter requiring addition of methanol to be observed (20). The 77 K multiline pattern is irregular and more similar in overall width to the S_2 multiline. Addition of 2.5% ethanol broadens the signal slightly.

DISCUSSION

Although the observation of the S_1 split signal requires the use of highly active, PSI free, PSII preparations, an initial question to be answered is why has this signal not been

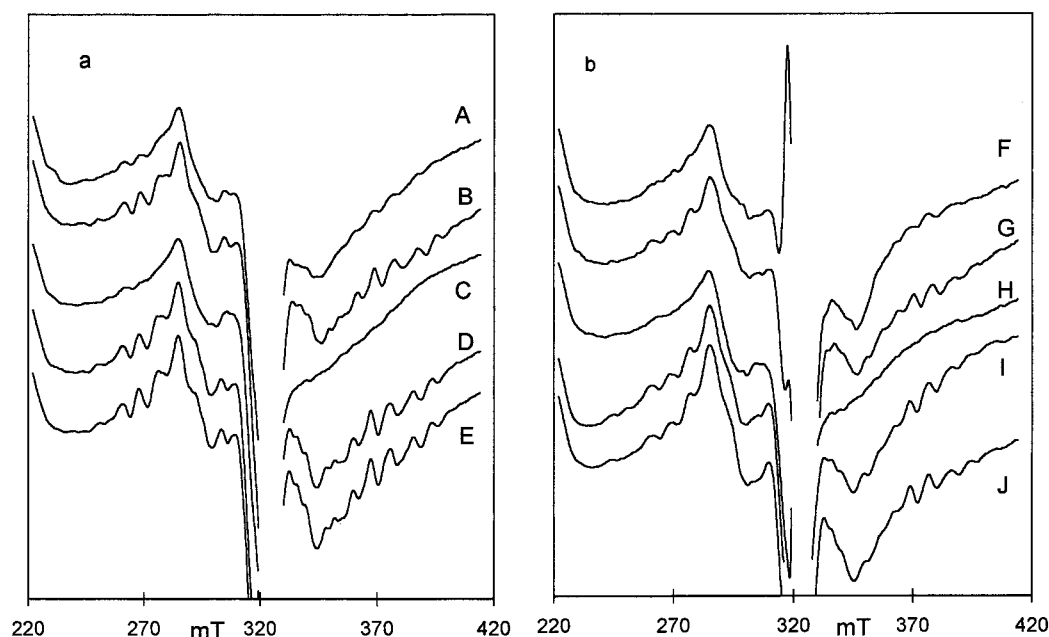


FIGURE 7: EPR spectra showing the effect of 2.5% ethanol on the S₁ split signal and generation of a multiline signal. The sample of pea PSII membranes (9.6 mg of Chl/mL) contained 1 mM DCBQ and either 2.5% ethanol (left box) or no further addition (right box). It was poised in the S₁ state following dark adaptation as given in Materials and Methods. (A, F) Illuminated at 6.7 K in the spectrometer. (B, G) After illumination at 77 K with <700 nm light for 15 min. (C, H) Dark-adapted sample. (D, I) Sample as in (B) the next day after reillumination at 77 K with <700 nm light for 15 min to restore the decayed signal. (E, J) Sample as in (D, I) after further illumination with white light (containing IR) for 5 min at 77 K. EPR conditions: temperature 6.7 K, modulation amplitude 2 mT, and microwave power 10 mW.

observed before given the many EPR studies of PSII? The answer is that there has not been a systematic attempt to see this kind of signal in PSII and it has probably been overlooked. In many previous PSII EPR studies in the literature, the effect of illumination is not measured at such temperatures. Also in many studies a larger modulation amplitude is used, which may result in the S₁ split signal (~65 G splitting for the central peaks) not being resolved from the large $g = 2$ peak of Y_D[•] and other secondary electron donors. There are, however, a few reports of similar signals in PSII. Rutherford (60, 61) reported a signal at $g = 2.045$ following illumination of PSII membranes that was lost on bicarbonate depletion and had properties distinct from Qa^{•-}. It was not characterized further, and it is possible that this is the same signal as discussed here although the illumination was performed at 77 K. Two groups, Beck and Brudvig (62) and Sivaraja and Dismukes (63, 64), reported a $g = 2.1$ signal in detailed EPR investigations of the effect of hydroxylamine on PSII. The signals reported in refs 62–64 are not identical to the S₁ split signal and required different conditions to be observed. The $g = 2.1$ signal has a different line shape and peak g -value, requiring a specific hydroxylamine treatment and then trapping by 200 K illumination to be detected. The S₁ split signal is found only on illumination below about 20 K and decays rapidly when illumination is stopped. It is now clear that the specific hydroxylamine treatment causes reduction of PSII first to S₀, then S₋₁, and then to lower redox states. The EPR signal for S₀ was first detected using similar treatments (20). A manuscript in preparation will describe experiments which investigate the broad radical signals from interactions when the Mn cluster is in S₀ and S₋₁ states.

Having detected the new signal, it is then necessary to establish whether the S₁ split signal originates from the electron donors or electron acceptors of PSII and from an

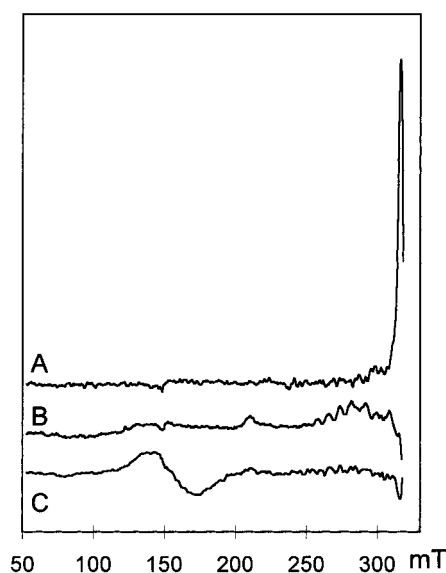


FIGURE 8: EPR spectra showing the three types of signals obtained by the different illumination conditions in this study. Spinach PSII membranes (8 mg of Chl/mL) containing 0.5 mM PPBQ dark-adapted to the S₁ state as given in Materials and Methods. These spectra represent the effect of successive illuminations, first at 10 K, then 77 K with <700 nm light, and then 77 K with unfiltered white light (containing IR). (A) Illuminated at 10 K minus dark-adapted spectrum showing S₁ split signal produced by illumination in the cavity at 10 K. (B) Illuminated at 77 K with <700 nm light for 15 min minus dark-adapted spectrum showing the 77 K multiline signal. (C) Illuminated at 77 K with unfiltered white light (containing IR) for 5 min minus illuminated at 77 K with <700 nm light showing $g = 4.1$ obtained with light containing IR. EPR conditions: temperature (A) 10 K and (B, C) 6.7 K, modulation amplitude 2 mT, and microwave power 10 mW.

electron transfer or an IR-induced transition. One explanation considered for our results was that <20 K illumination was forming an S₀Y_Z[•] state from S₁, in a similar way to the

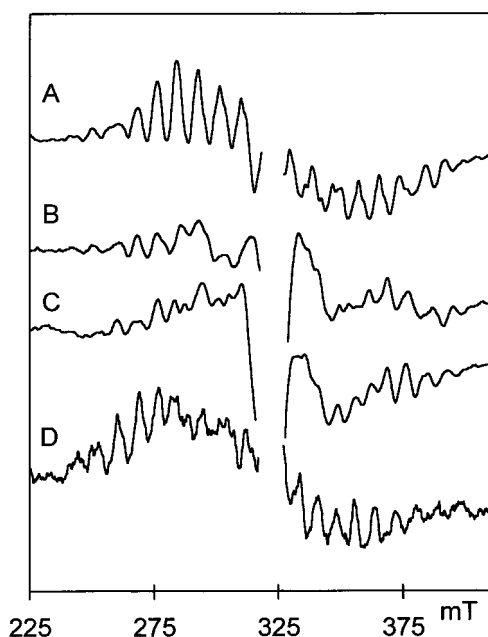


FIGURE 9: EPR spectra comparing multiline line shapes. All spectra are from pea PSII. (A) S_2 multiline. 200 K illuminated minus S_1 dark difference spectrum. (B) 77 K multiline. Sample as in Figure 7. 77 K illuminated minus S_1 dark difference spectrum. The sample contained 1 mM DCBQ and 2.5% ethanol. (C) 77 K multiline. Sample as in Figure 7. 77 K illuminated minus S_1 dark difference spectrum. The sample contained 1 mM DCBQ. (D) S_0 multiline. Sample prepared as in ref 20 by reduction from S_1 using hydroxylamine. The spectrum shown is the difference between a sample containing 1.5% methanol and a non-methanol-treated sample. EPR conditions as in Figure 7.

proposed formation of $S_2Y_Z^{\bullet}$ from S_3 caused by IR illumination (33). However, the formation of the multiline signal attributed to S_2 , both on warming a <20 K illuminated sample in the dark and by direct illumination with <700 nm light, demonstrates that a charge separation and forward electron transfer are occurring.

The relatively rapid decay of the S_1 split signal on cessation of illumination at <20 K, restoring the state before illumination, suggests that a recombination reaction occurs. The rapid recombination reaction following illumination (Figure 4) contrasts with the very slow (days) recombination of $Qa^{\bullet-}$ with Y_D^{\bullet} , the multiline or $g = 4.1$ forms of S_2 , Cyt b -559, and Chl Z^+ (1–3). The detailed study of the carotenoid radical in PSII (53–55) is relatively recent, and it is possible that this radical could interact with the Mn cluster to give the S_1 split signal. There are differences in the reported decay kinetics from different groups, and the radical has been mainly studied in Mn-depleted PSII where it is more easily detected. In ref 54 the decay of the carotenoid radical at 6 and 30 K in Mn-depleted samples is multiphasic with an overall decay of $\sim 30\%$ in 100 min and with even the fastest component being much slower than observed for the S_1 split radical. However, in ref 55 using oxygen-evolving PSII oxidized with ferricyanide, the decay rates reported were faster (seconds) at 20 K than those of the S_1 split radical. This suggests that the S_1 split signal could involve the $Car^{\bullet+}$ radical. However, EPR studies of the $Car^{\bullet+}$ radical (53–55) have shown a nearly isotropic spectrum near $g = 2$ with no indication of interaction with a transition metal. If carotenoid were involved in the S_1 split signal, then the results presented here suggest that S_1 can

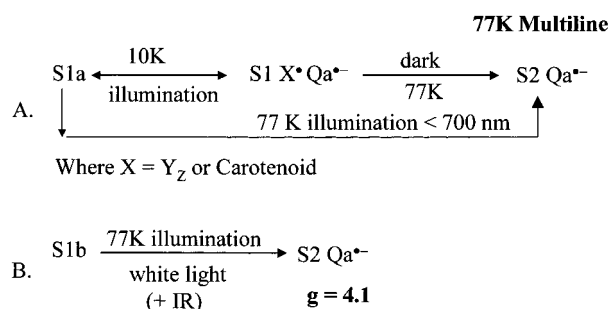
be oxidized by the $Car^{\bullet+}$ radical. The $Car/Car^{\bullet+}$ redox couple has an estimated redox potential of ~ 1 V (65).

Illumination below 200 K is known to restrict turnover of PSII to one turnover with Qa or Fe^{3+} (when present) acting as terminal electron acceptors. This means that the electron is returning from I^- , Fe^{2+} , or $Qa^{\bullet-}$. I^- is very difficult to detect in PSII; electron donors are unable to compete at cryogenic temperatures with the very fast $P680^+ I^-$ back-reaction. Photoaccumulation at >200 K is required to produce I^- , using reductants as electron donors to PSII. If it were possible to form I^- in addition to $Qa^{\bullet-}$ during illumination at <20 K, then a split $g = 2$ from the weak interaction $I^- Qa^{\bullet-} Fe^{2+}$ should occur. However, $I^- Qa^{\bullet-}$ formation in nonchemically reduced samples has not been observed in EPR studies of oxygen-evolving PSII, and the interaction seen in the present study does not have the very rapid decay characteristics expected, suggesting I^- is not present.

An interaction involving $Qb^{\bullet-}$ and $Qa^{\bullet-}$ could be involved in formation of the S_1 split signal. DCBQ does have a relatively stable semiquinone state (66), and we have used FCCP previously to increase the level of $Qb^{\bullet-}$ in PSII membranes in studies showing that an EPR signal observed near $g = 1.6$ in PSII was from the state $Qa^{\bullet-} Fe^{2+} Qb^{\bullet-}$ (67, 68). The $Qa^{\bullet-} Fe^{2+} Qb^{\bullet-}$ state does not decay rapidly (67, 68), and the observation of the S_1 split signal in samples containing PPBQ or DCMU (Figure 2) suggests that $Qb^{\bullet-}$ is not involved. Amounts of $Qb^{\bullet-}$ are expected to be minimal in these samples as DCMU displaces Qb , and $PPBQb^{\bullet-}$ formed on electron transfer is not stable as it has a high redox potential, oxidizing the non-heme iron, forming $PPBQH_2$. The variety of conditions also seems to rule out the involvement of the non-heme iron. It is therefore concluded that (1) it is highly unlikely that the S_1 split signal is from an interaction between electron acceptors and (2) $Qa^{\bullet-}$, which partially decays as the S_1 split signal decays, is the electron acceptor species involved in charge recombination with the S_1 split signal. It is well-known that effects due to structural changes in the quinone-binding region can be transmitted to the electron donors to PSII (1–3). From our studies, the occupation of the Qb site (by $Qb^{\bullet-}$, an exogenous quinone, or inhibitor) does seem important in poisoning PSII in the correct structural configuration to observe the S_1 split signal.

The decay of the S_1 split signal is biphasic, and we show that, in addition to recombination, a forward electron transfer to form a multiline signal can occur. The increased yield from the treatments shown above such as FCCP and exogenous quinones is at least partially explained by their oxidation of Cyt b -559, probably restricting competition between secondary donors and the species oxidized to form the S_1 split signal. Among the electron donors, the back-reaction between $P680^+$ and $Qa^{\bullet-}$ is much faster (milliseconds) (69) than that seen in this study, while the back-reaction of $Qa^{\bullet-}$ with S_2 states is far slower (1–3, 17). Both the characteristics of the S_1 split signal and its kinetics do however closely resemble those of the interaction between Y_Z^{\bullet} and the Mn cluster in the S_2 state. Although this study does not prove that Y_Z^{\bullet} is involved, from the earlier discussion only carotenoid can also possibly fit the properties observed. We therefore suggest that it is more likely that the S_1 split signal arises from an interaction between Y_Z^{\bullet} formed by illumination and the S_1 state of the WOC, as Y_Z

Scheme 1



is a known intermediate between P680 and the S-states. The conditions required to observe the signal are those known to favor the paramagnetic forms of S₁ (23–26), while treatments such as methanol or ethanol that remove paramagnetic S₁ states also prevent the S₁ split signal from being formed (Figure 7).

The yield of signal does vary from preparation to preparation in both spinach and pea PSII, as well as by choice of cryoprotectant or electron acceptor. This undefined heterogeneity was also seen in studies of the IR-induced *g* = 4.1 S₂ signal, 20–70% of PSII responding to IR illumination (35). Comparison of the conditions tested in this study and ref 35 suggests that they complement each other and show that we are observing those centers not sensitive to IR illumination. Even allowing for the contribution of secondary electron donors, the WOC itself therefore exhibits heterogeneity and is sensitive to additions such as cryoprotectants and alcohols, in that different signals are observed in various S-states under different conditions. This heterogeneity was also demonstrated in the difficulty found in reproducing the original observation of an S₁ parallel EPR signal (23) until the correct conditions were found (24).

Our conclusions can be summarized by Scheme 1. We propose that there are two slightly different S₁ states that can be resolved by their EPR characteristics.

The S₁ state is known to have different electronic arrangements, which result in the different EPR signals (23–26) and are most easily explained, as for S₂ state, as different arrangements of the Mn³⁺ and Mn⁴⁺ ions of the cluster (70). The configuration is affected by relatively small changes that could be caused, for example, by the presence or absence of a proton or H₂O/OH[−] binding as ligands to the Mn cluster. The absence of an effect of IR illumination on the 77 K multiline indicates that the Mn³⁺ atom thought to be affected by IR may be the one that has been oxidized at low temperature in these centers.

Our results confirm that the S₁ to S₂ step can occur at temperatures that preclude proton or hydrogen atom movements, in a substantial proportion of centers, in our preparations. Y_Z is oxidized fast, the fast nanosecond phase at physiological temperatures being observed in a similar proportion (40–50%) of reaction centers (1–6) as that estimated here for the ability to form the S₁ split signal. The transition is almost insensitive to H/D substitution and has a low activation barrier (see refs 1–3 and 17). These are characteristic of electron-transfer reactions, and in our view the rate limitation of proton transfer is removed in native PSII but restored by structural change in cofactor-depleted PSII. Our results require X (Y_Z or carotenoid) to

operate as a pure electron transfer cofactor in this portion of centers. Reduced carotenoid is not protonated, and if X = Y_Z, it should also not be formally protonated in the reduced form. We believe that the predicted substantial difference in pK_a's between Y_Z and possible nearby hydrogen bond donors such as D1 histidine 190, D1 glutamate 189, and D1 glutamine 165 can be decreased by the protein environment to effectively create a tyrosinate in the reduced form of Y_Z, the proton being shared by two or more nearby amino acids in low-barrier hydrogen bonds. Upon oxidation of Y_Z the proton in the hydrogen bond would move toward the base, a process that could still occur at liquid helium temperatures. This would be a delicate mechanism, the electrostatic balance being easily shifted by slight perturbations to the PSII center, which would account for the variation in the proportion of centers having the S₁ split signal. The balance would be easily destroyed by more substantial changes, for example, involving removal of manganese or calcium cofactors. Among cryoprotectants, glycerol has already been shown to restore the pattern of proton release observed in thylakoids, an effect thought to be through stabilization of the PSII structure relative to sucrose (71). That glycerol increases the yield of the S₁ split signal seems to correlate with the absence of a requirement for a deprotonation on the S₁ to S₂ step. However, the increased yield may alternatively be due to the ability of glycerol to increase the amount of oxidized Cyt *b*-559 in dark-adapted samples (72).

SUMMARY

In recent years a number of new EPR signals have been characterized that give us probes of the turnover of the WOC. These have included broad radical signals from interaction of the Y_Z component with the Mn cluster. These have the potential to give important information about changes in the Mn cluster during S-state turnover. We now show the characterization of a new signal we attribute to the interaction between the paramagnetic S₁ state and Y_Z[•] or Car^{•+} as an intermediate between the S₁ and S₂ states. The results suggest that a substantial number of centers are able to operate the S₁ to S₂ step at very low temperatures, confirming the unusual temperature profile of this step. Further work using pulsed EPR will be required to confirm that Y_Z[•] or Car^{•+} is involved in the S₁ split signal as shown for the S₂Y_Z[•] interaction (47).

ACKNOWLEDGMENT

We thank Vasili Petrouleas and Nikos Ioannidis for helpful discussion.

REFERENCES

- Diner, B. A., and Babcock, G. T. (1996) in *Oxygenic Photosynthesis: The Light Reactions* (Ort, D. R., and Yocum, C. F., Eds.) pp 213–247, Kluwer Academic Publishers, Dordrecht, The Netherlands.
- Britt, R. D. (1996) in *Oxygenic Photosynthesis: The Light Reactions* (Ort, D. R., and Yocum, C. F., Eds.) pp 137–164, Kluwer Academic Publishers, Dordrecht, The Netherlands.
- Nugent, J. H. A. (1996) *Eur. J. Biochem.* 237, 519–531.
- Lavergne, J., and Junge, W. (1993) *Photosynth. Res.* 38, 279–296.
- Schilstra, M. J., Rappaport, F., Nugent, J. H. A., Barnett, C. J., and Klug, D. R. (1998) *Biochemistry* 37, 3974–3981.
- Christen, G., Seeliger, A., and Renger, G. (1999) *Biochemistry* 38, 6082–6092.

7. Nugent, J. H. A., Rich, A. M., and Evans, M. C. W. (2001) *Biochim. Biophys. Acta* 1503, 138–146.
8. Hoganson, C. W., and Babcock, G. T. (1999) in *Biological Processes in Metal Ions in Biological Systems* (Sigel, A., and Sigel, H., Eds.) Vol. 37, pp 613–656, Marcel Dekker, New York.
9. Hoganson, C. W., Lydakis-Simantiris, N., Tang, X.-S., Tommos, C., Warncke, K., Babcock, G. T., Diner, B. A., McCracken, J., and Styring, S. (1995) *Photosynth. Res.* 46, 177–184.
10. Hoganson, C. W., and Babcock, G. T. (1997) *Science* 277, 1953–1956.
11. Force, D. A., Randall, D. W., and Britt, R. D. (1997) *Biochemistry* 36, 12062–12070.
12. Haumann, M., and Junge, W. (1996) in *Oxygenic Photosynthesis: The Light Reactions* (Ort, D. R., and Yocum, C. F., Eds.) pp 165–192, Kluwer Academic Publishers, Dordrecht, The Netherlands.
13. Limburg, J., Szalai, V. A., and Brudvig, G. W. (1999) *J. Chem. Soc., Dalton Trans.*, 1353–1361.
14. Haumann, M., and Junge, W. (1999) *Biochim. Biophys. Acta* 1411, 86–91.
15. Joliot, P., Barbieri, G., and Chabaud, R. (1969) *Photochem. Photobiol.* 10, 309–329.
16. Kok, B., Forbush, B., and McGloin, M. (1970) *Photochem. Photobiol.* 11, 457–475.
17. Debus, R. J. (1992) *Biochim. Biophys. Acta* 1102, 269–352.
18. Messinger, J., Badger, M., and Wydrzynski, T. (1995) *Proc. Natl. Acad. Sci. U.S.A.* 92, 3209–3213.
19. Hillier, W., Messinger, J., and Wydrzynski, T. (1998) *Biochemistry* 37, 16908–16914.
20. Messinger, J., Nugent, J. H. A., and Evans, M. C. W. (1997) *Biochemistry* 36, 11055–11060.
21. Ahrling, K., Peterson, S., and Styring, S. (1997) *Biochemistry* 36, 13148–13152.
22. Messinger, J., Robblee, J., Yu, W. O., Sauer, K., Yachandra, V. K., and Klein, M. P. (1997) *J. Am. Chem. Soc.* 119, 11349–11350.
23. Dexheimer, S. L., and Klein, M. P. (1992) *J. Am. Chem. Soc.* 114, 2821–2826.
24. Yamauchi, T., Mino, H., Matsukawa, T., Kawamori, A., and Ono, T. (1997) *Biochemistry* 36, 7520–7526.
25. Campbell, K. A., Peloquin, J. M., Pham, D. P., Debus, R. J., and Britt, R. D. (1998) *J. Am. Chem. Soc.* 120, 447–448.
26. Campbell, K. A., Gregor, W., Pham, D. P., Peloquin, J. M., Debus, R. J., and Britt, R. D. (1998) *Biochemistry* 37, 5039–5045.
27. Dismukes, G. C., and Siderer, Y. (1981) *Proc. Natl. Acad. Sci. U.S.A.* 78, 274–278.
28. Hansson, O., and Andreasson, L. E. (1982) *Biochim. Biophys. Acta* 679, 261–268.
29. Casey, J. L., and Sauer, K. (1984) *Biochim. Biophys. Acta* 767, 21–28.
30. Zimmermann, J. L., and Rutherford, A. W. (1984) *Biochim. Biophys. Acta* 767, 160–167.
31. Nugent, J. H. A., Turconi, S., and Evans, M. C. W. (1997) *Biochemistry* 36, 7086–7096.
32. Matsukawa, T., Mino, H., Yoneda, D., and Kawamori, A. (1999) *Biochemistry* 38, 4072–4077.
33. Ioannidis, N., and Petrouleas, V. (2000) *Biochemistry* 39, 5246–5254.
34. Boussac, A., Girerd, J.-J., and Rutherford, A. W. (1996) *Biochemistry* 35, 6984–6989.
35. Boussac, A. (1997) *J. Biol. Inorg. Chem.* 2, 580–585.
36. Boussac, A., Un, S., Horner, O., and Rutherford, A. W. (1998) *Biochemistry* 37, 4001–4007.
37. Boussac, A., and Rutherford, A. W. (2000) *Biochim. Biophys. Acta* 1457, 145–156.
38. MacLachlan, D. J., Nugent, J. H. A., Warden, J. T., and Evans, M. C. W. (1994) *Biochim. Biophys. Acta* 1188, 325–334.
39. Peloquin, J. M., Campbell, K. A., and Britt, R. D. (1998) *J. Am. Chem. Soc.* 120, 6840–6841.
40. Dorlet, P., Di Valentin, M., Babcock, G. T., and McCracken, J. L. (1998) *J. Phys. Chem. B* 102, 8239–8247.
41. Lakshmi, K. V., Eaton, S. S., Eaton, G. R., Frank, H. A., and Brudvig, G. W. (1998) *J. Phys. Chem. B* 102, 8327–8335.
42. Boussac, A., Zimmermann, J. L., and Rutherford, A. W. (1989) *Biochemistry* 28, 8984–8989.
43. Sivaraja, M., Tso, J., and Dismukes, G. C. (1989) *Biochemistry* 28, 9459–9464.
44. Ono, T., and Inoue, Y. (1989) *Biochim. Biophys. Acta* 973, 443–449.
45. Hallahan, B. J., Nugent, J. H. A., Warden, J. T., and Evans, M. C. W. (1992) *Biochemistry* 31, 4562–4573.
46. MacLachlan, D. J., and Nugent, J. H. A. (1993) *Biochemistry* 32, 9772–9780.
47. Gilchrist, M. L., Ball, J. A., Randall, D. W., and Britt, R. D. (1995) *Proc. Natl. Acad. Sci. U.S.A.* 92, 9545–9549.
48. Nugent, J. H. A., and Turconi, S. (1995) in *Photosynthesis: from Light to Biosphere* (Mathis, P., Ed.) Vol. II, pp 455–458, Kluwer Academic Publishers, The Netherlands.
49. Nugent, J. H. A., and Evans, M. C. W. (1998) in *Photosynthesis: Mechanisms and Effects* (Garab, G., Ed.) Vol. II, pp 1379–1382, Kluwer Academic Publishers, Dordrecht, The Netherlands.
50. Ford, R. C., and Evans, M. C. W. (1983) *FEBS Lett.* 160, 159–163.
51. Porra, R. J., Thompson, W. A., and Kriedemann, P. E. (1989) *Biochim. Biophys. Acta* 975, 384–394.
52. De Paula, J. C., Innes, J. B., and Brudvig, G. W. (1985) *Biochemistry* 24, 8114–8120.
53. Hanley, J., Deligiannakis, Y., Pascal, A., Faller, P., and Rutherford, A. W. (1999) *Biochemistry* 38, 8189–8195.
54. Tracewell, C. A., Cua, A., Stewart, D. H., Bocian, D. F., and Brudvig, G. W. (2001) *Biochemistry* 40, 193–203.
55. Faller, P., Pascal, A., and Rutherford, A. W. (2001) *Biochemistry* 40, 6431–6440.
56. Nugent, J. H. A. (2001) *Biochim. Biophys. Acta* 1504, 288–298.
57. Evans, M. C. W., Rich, A. M., and Nugent, J. H. A. (2000) *FEBS Lett.* 477, 113–117.
58. Cua, A., Stewart, D. H., Reifler, M. J., Brudvig, G. W., and Bocian, D. F. (2000) *J. Am. Chem. Soc.* 122, 2069–2077.
59. Baxter, R., Krausz, E., Wydrzynski, T., and Pace, R. J. (1999) *J. Am. Chem. Soc.* 121, 9451–9452.
60. Vermaas, W. F. J., and Rutherford, A. W. (1984) *FEBS Lett.* 175, 243–247.
61. Rutherford, A. W. (1985) *Biochim. Biophys. Acta* 807, 189–201.
62. Beck, W. F., and Brudvig, G. W. (1987) *Biochemistry* 26, 8285–8295.
63. Sivaraja, M., and Dismukes, G. C. (1988) *Biochemistry* 27, 3467–3475.
64. Sivaraja, M., and Dismukes, G. C. (1988) *Biochemistry* 27, 6297–6306.
65. Edge, R., Land, E. J., McGarvey, D. J., Burke, M., and Truscott, T. G. (2000) *FEBS Lett.* 471, 125–127.
66. Hoganson, C. W., and Babcock, G. T. (1988) *Biochemistry* 27, 5848–5855.
67. Hallahan, B. J., Ruffle, S. V., Bowden, S. J., and Nugent, J. H. A. (1991) *Biochim. Biophys. Acta* 1059, 181–188.
68. Corrie, A. R., Nugent, J. H. A., and Evans, M. C. W. (1991) *Biochim. Biophys. Acta* 1057, 384–390.
69. Nugent, J. H. A., Diner, B. A., and Evans, M. C. W. (1982) *Biochim. Biophys. Acta* 682, 106–114.
70. Peloquin, J. M., and Britt, R. D. (2001) *Biochim. Biophys. Acta* 1503, 96–111.
71. Haumann, M., Hundelt, M., Jahns, P., Chroni, S., Bogershausen, O., Ghanotakis, D., and Junge, W. (1997) *FEBS Lett.* 410, 242–248.
72. Visser, J. W. M., Rijgersberg, C. P., and Gast, P. (1977) *Biochim. Biophys. Acta* 460, 36–46.